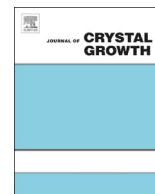




ELSEVIER

Contents lists available at ScienceDirect

Journal of Crystal Growth

journal homepage: [www.elsevier.com/locate/crysgro](http://www.elsevier.com/locate/crysgro)

# Self-organized InAs/InAlGaAs quantum dots as dislocation filters for InP films on (001) Si

Bei Shi, Qiang Li, Kei May Lau\*

Department of Electronic and Computer Engineering, Hong Kong University of Science and Technology, Clear Water Bay, Kowloon, Hong Kong

## ARTICLE INFO

Communicated by Dr. T.F. Kuech

## Keywords:

- A1. Defects
- A3. Metalorganic chemical vapor deposition
- A3. Quantum dots
- B2. Semiconducting III–V materials

## ABSTRACT

We report the effects of multi-layer InAs/InAlGaAs quantum dots (QDs) inserted as dislocation filters into an InP thin film epitaxially grown on (001) Si substrates by metalorganic chemical vapor deposition. The surface of the InP-on-Si template using 500 nm GaAs as an intermediate buffer is anti-phase-boundary-free. With the QD filters introduced, a four-fold reduction of dislocation density, to the order of  $3.2 \times 10^8/\text{cm}^2$  was achieved, based on observation of large-area cross-sectional transmission electron microscopy (TEM). The dislocation filtering mechanism was further analyzed through zoomed-in TEM images. Bending or coalescence of threading dislocations in the presence of the strain field induced by the QD filters led to annihilation reactions. Moreover, the improved crystalline quality of the InP above the dislocation filters was manifested by enhanced intensities and reduced full-width at half-maximum values in the statistical room temperature photoluminescence spectra. These results indicate that introducing QD dislocation filters could be beneficial for the epitaxial growth of high quality 1.55  $\mu\text{m}$  band lasers on a Si manufacturing platform.

## 1. Introduction

Heteroepitaxy of III–V compound semiconductors on Si has been an enduring pursuit due to its potential applications in silicon photonics, optical interconnections and advanced CMOS technologies [1]. InP-based alloys offer a favorable wavelength (1.55  $\mu\text{m}$  C-band) for inter/intra-chip optical interconnects and long-haul fiber communication systems [2]. However, direct epitaxy of InP on Si faces the fundamental challenges associated with the large mismatch in lattice constants ( $\sim 8\%$ ) and thermal expansion coefficients ( $\sim 50\%$ ) [3]. The lattice mismatch gives rise to a high density of threading dislocations (TDs) in the order of  $10^9$ – $10^{10}/\text{cm}^2$ , which seriously degrade device performance and reliability. Formation of anti-phase-domains (APDs) is also common when III–V materials are grown on silicon.

In the past decades, various approaches have been developed focusing on addressing the dislocation issues brought about by III–V hetero-epitaxy on Si. Techniques including thermal cycle growth [4], compositional graded buffers [5,6], patterned growth [7–9], strained-layer superlattice (SLS) [10,11], and epitaxial lateral overgrowth (ELOG) [12,13] have been adopted. Theoretically, strained layers are effective in bending TDs, thereby increasing dislocation annihilation or transportation to the edge of the sample. Compared with conventional two-dimensional SLS, self-assembled InAs quantum dots (QDs) produced by Stranski-Krastanow (SK) growth mode provide a larger strain

field and stronger Peach-Koehler force, thus potentially offering more effective dislocation filtering capability. The dislocation filtering effect of InAs/GaAs QDs has been proven in the GaAs-on-Si hetero-epitaxy [14,15]. Yet for InP-on-Si system, which is more challenging in terms of growth due to a larger lattice mismatch and a higher dislocation density, there has been no investigation of utilizing three dimensional (3D) QDs as dislocation filters.

In this paper, we investigate the dislocation filtering effects of 7-layer InAs/InAlGaAs QDs inserted into an InP thin film epitaxially grown on (001) Si. Improved crystalline quality of the InP layer above the filters was observed, together with a smoother InP surface morphology. This study offers an approach to facilitate defect reduction in InP-based materials epitaxially grown on Si, which could be useful to the monolithic integration of telecom wavelength photonic components on the industrial-standard Si platform.

## 2. Experimental details

The InP-on-Si material growth was performed in an AIX-200/4 metalorganic chemical vapor deposition (MOCVD) system equipped with a Laytec EpiRAS setup for in-situ growth spectral reflectance monitoring. A 4-in. (001) Si substrate was first cleaned using  $\text{NH}_3\text{OH}:\text{H}_2\text{O}_2:\text{H}_2\text{O}=1:1:5$  (RCA1) for 10 min and then dipped in 1% diluted hydrofluoric acid for 1 min to remove the native oxide.

\* Corresponding author.

E-mail address: [ekmlau@ust.hk](mailto:ekmlau@ust.hk) (K.M. Lau).<http://dx.doi.org/10.1016/j.jcrysgro.2016.10.089>

Received 5 September 2016; Received in revised form 25 October 2016; Accepted 30 October 2016

Available online xxx

0022-0248/ © 2016 Elsevier B.V. All rights reserved.

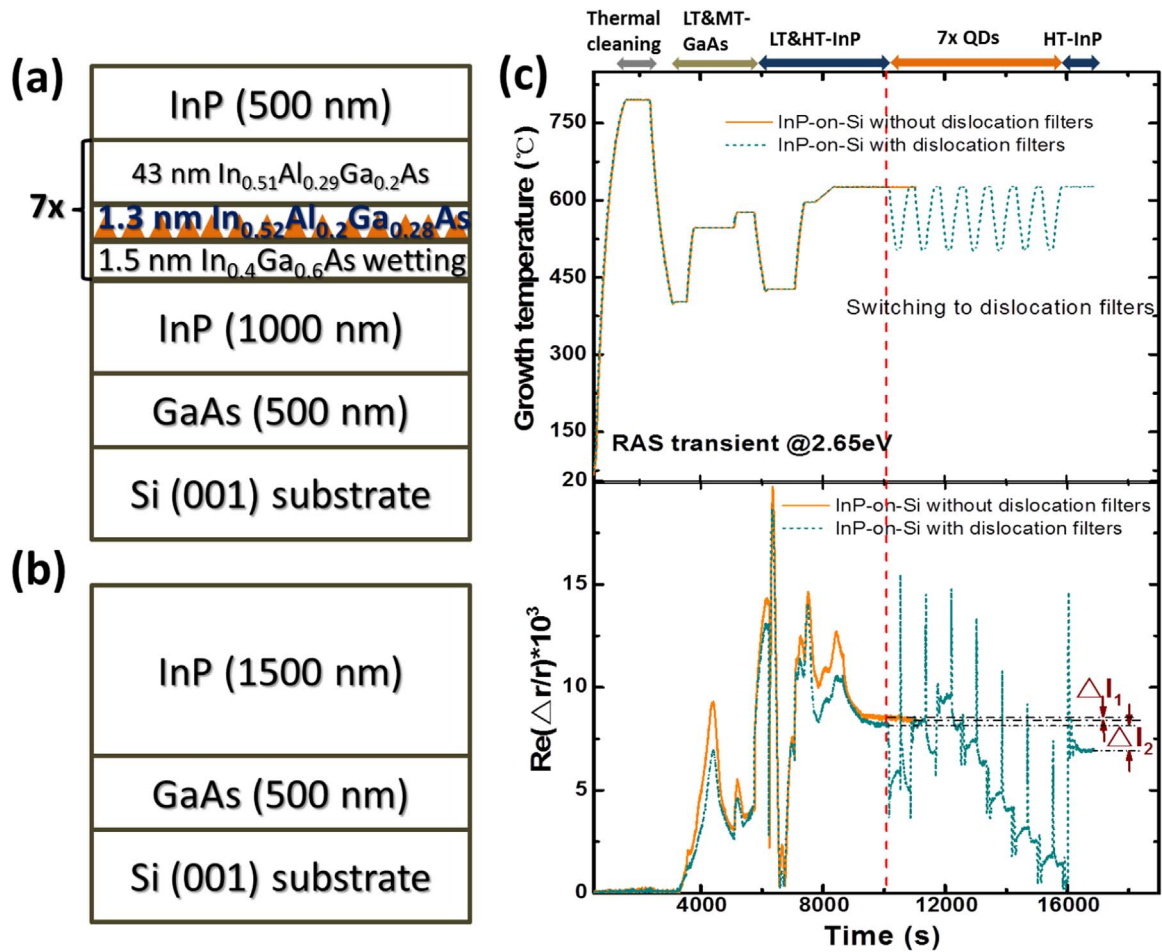


Fig. 1. Schematic diagram of InP-on-Si template (a) with and (b) without multi-layer QD dislocation filters; (c) In-situ growth signal of InP-on-Si with and without QD filters.

Afterwards, the Si wafer was annealed in the MOCVD reactor at 800 °C for 15 min for further deoxidation. A GaAs intermediate buffer was deposited by the two-step growth method [16]. Specifically, a thin low-temperature (LT) GaAs nucleation layer was grown to form dense and uniform GaAs islands on Si, followed by a 500 nm high-temperature (HT) GaAs main layer to improve the material quality. The 1- $\mu\text{m}$ -thick

InP was grown on top in a similar two-step method and 7-layer InAs/InAlGaAs QDs were deposited subsequently on the relatively flat and stable InP front [17]. Prior to the InAs QDs deposition, a ~1.5 nm  $\text{In}_{0.4}\text{Ga}_{0.6}\text{As}$  wetting layer was grown at 630 °C, and then cooled down to 510 °C for QDs growth. The QDs were grown for 10 s with a deposition amount of 3.6 monolayer (ML) and a V/III of ~0.4. After in-

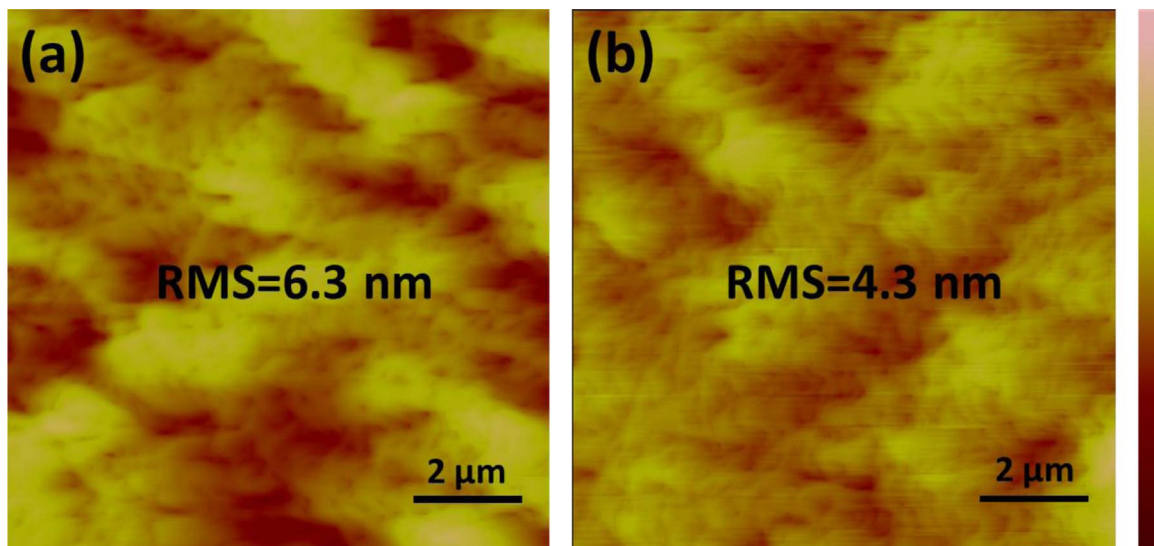
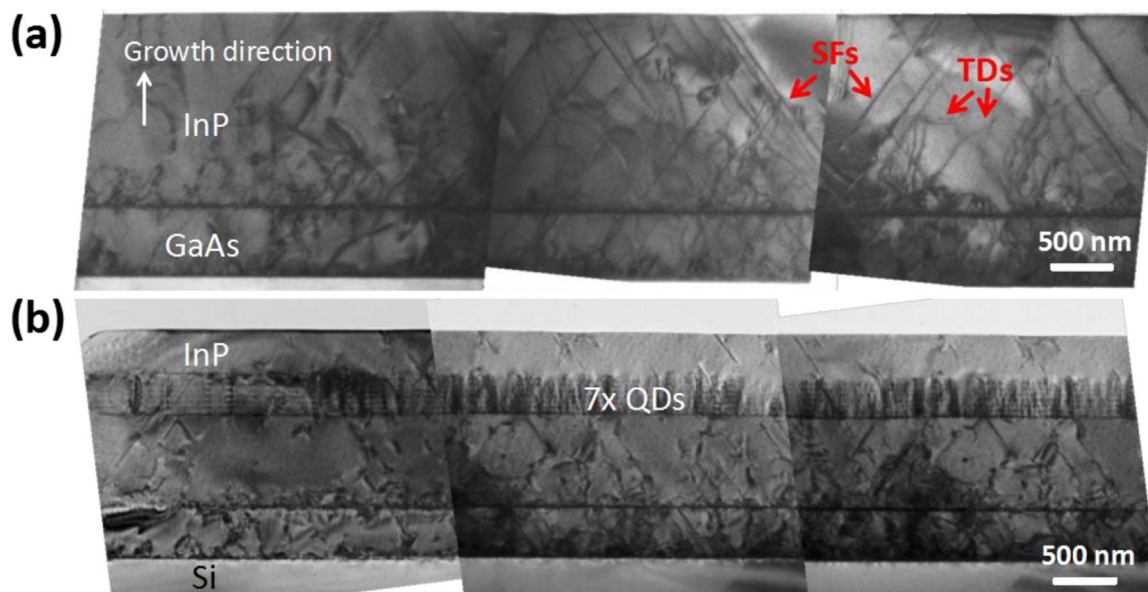


Fig. 2. Typical  $10 \times 10 \mu\text{m}^2$  AFM images of InP-on-Si surface (a) without and (b) with dislocation filters. The RMS values for these two samples are 6.3 nm and 4.3 nm, respectively. The color scale is 60 nm.



**Fig. 3.** Large-area XTEM images of the InP-on-Si (a) without QDs (total width of 8.94  $\mu\text{m}$ ) and (b) with QD filter layers (total width of 8.49  $\mu\text{m}$ ).

situ annealing in tertiarybutylarsine (TBA) ambient for 5 s, a thin LT-InAlGaAs first cap layer ( $\sim 1.3$  nm) was grown immediately to bury the QDs and another  $\sim 43$  nm HT-InAlGaAs second cap layer was deposited

at an elevated temperature of 630  $^{\circ}\text{C}$ . The structure was repeated for seven times to grow the 7-layer QD dislocation filters. Finally, the QDs were capped by a 500 nm HT-InP layer.

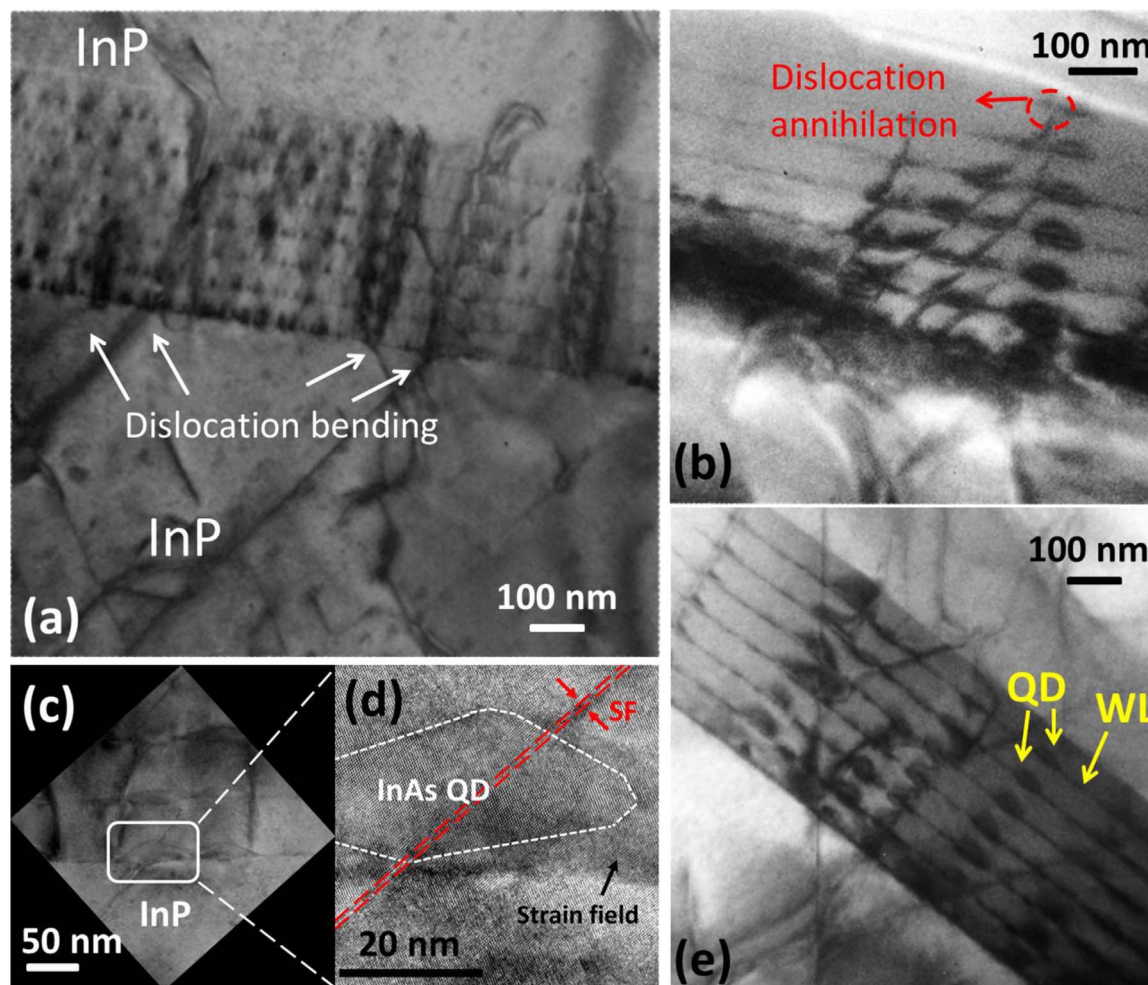


**Fig. 4.** Close-up XTEM view of the QD dislocation filter layers to illustrate (a) dislocation bending and (b) dislocation interaction and annihilation; (c) High-resolution image of the SFs penetrating through a large QD and (d) zoomed-in view of a diamond shaped QD as well as the strain field; (e) Close-up view of the vertically aligned QDs with the wetting layers (WLs) identified.

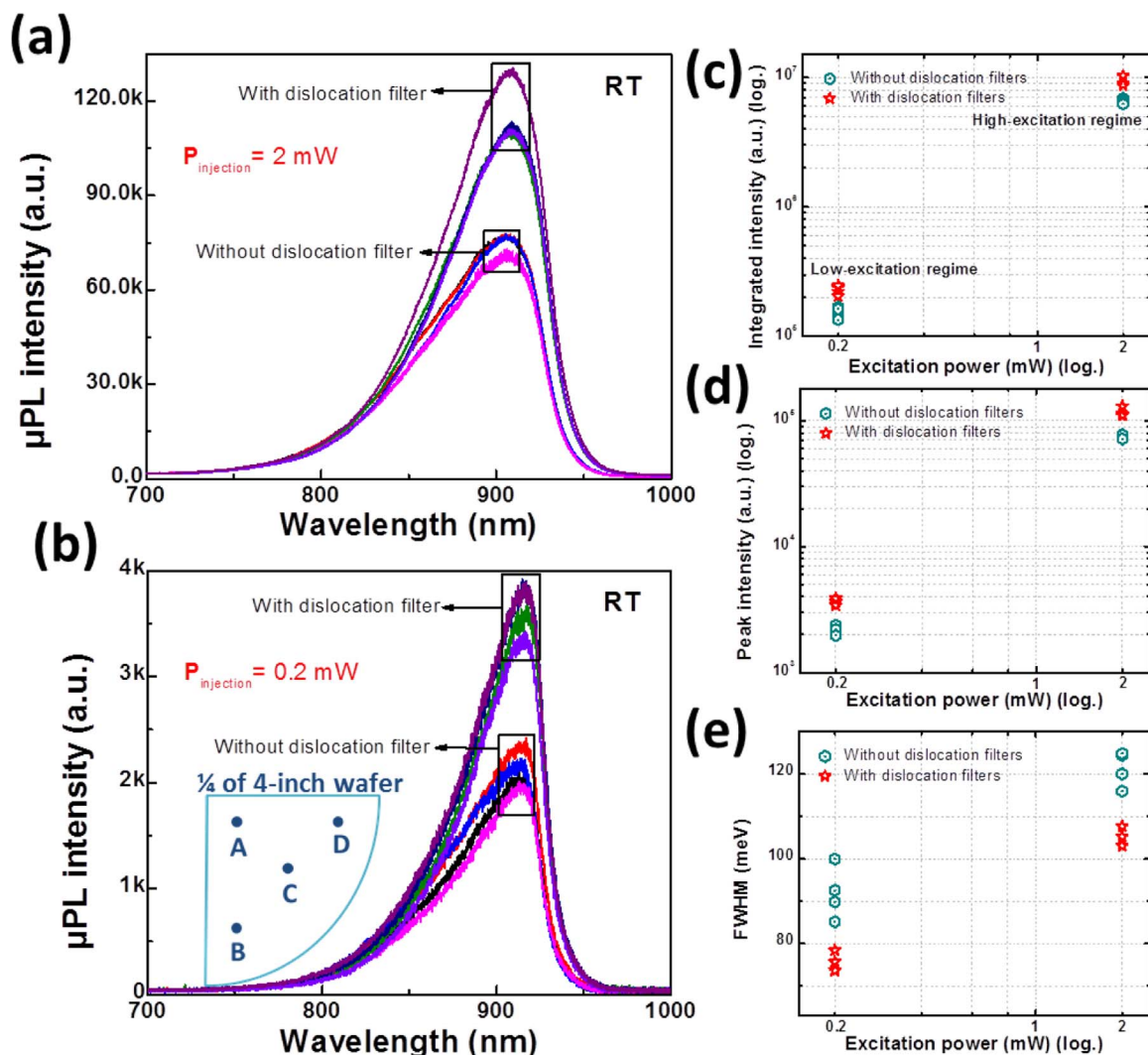


**Fig. 5.** (a)-(b) Statistical room-temperature power-dependent PL spectra of the InP-on-Si with and without QD dislocation filters at two different excitation power regimes over the quarter of 4-in. samples; (c) Extracted integrated intensity, (d) peak intensity and (e) FWHM of the two samples as a function of the excitation power..

The schematic diagram of the grown layers is illustrated in Fig. 1(a). For a fair evaluation of the dislocation filtering efficiency, another sample with the same thickness of InP and GaAs buffers was grown without any QDs insertion, as shown in Fig. 1(b). Fig. 1(c) compares the time-resolved reflectance anisotropy spectroscopy (RAS) signal of both samples, indicating surface morphology evolution of the InP-on-Si templates with and without the QD filters. The RAS transient energy was chosen at 2.65 eV, which is sensitive to the surface morphology and roughness [16]. Without the insertion of the QD dislocation filter, the RAS is rather flat with negligible intensity decrease ( $\Delta I_1$ ) during the final 500 nm InP layer. However, an obvious RAS intensity drop ( $\Delta I_2$ ) has been observed in the other sample after the insertion of 7-layer QDs. Qualitatively, the more significant RAS decrease reflects a less anisotropic surface morphology and thus a smoother surface. Moreover, the gradual and periodic decrease of the RAS during stacking of the multiple QDs was a good indication of an effective separation between each QD layer and an As-stabilized surface front prior to the subsequent QDs deposition. It has been observed that an increased time-resolved RAS signal during the stacking corresponds to a deteriorated surface quality [18].

### 3. Results and discussion

The surface morphologies of the two samples were inspected by

atomic force microscopy (AFM), as demonstrated in Fig. 2. Anti-phase-boundary (APB)-free surfaces were realized in both samples. With inserted dislocation filters, the root-mean-square (RMS) roughness was reduced from 6.3 to 4.3 nm, across a scan area of  $10 \times 10 \mu\text{m}^2$ . This observation is in consistent with the indication of the in-situ RAS signal. The better surface morphology of the InP-on-Si with the QDs insertion will be beneficial for upper active layers (quantum wells or quantum dots) growth, providing a smoother and sharper interface.

The dislocation filtering function of the multi-layer QDs was examined by cross-sectional transmission electron microscopy (XTEM). Taken along the [110] zone axis, a series of bright-field TEM images in Fig. 3 present the dislocation distribution in both samples. High density of TDs and stacking faults (SFs) were generated at the hetero-interface of the InP/GaAs and GaAs/Si. As shown in Fig. 3(a), these dislocations propagated toward the top surface of the InP without obvious interruption. Considering the XTEM specimen to be in the order of  $\sim 400 \text{ nm}$  [19], the dislocation density is estimated to be  $\sim 1.3 \times 10^9 \text{ cm}^{-2}$ . Owing to the insertion of the 7-layer InAs/InAlGaAs QDs, an evident dislocation bending and filtering effect can be noticed. From the montage of three successive TEM images in Fig. 3(b), the average dislocation density at the InP top surface is counted to be  $\sim 3.2 \times 10^8 \text{ cm}^{-2}$ , realizing a four-fold reduction compared to the sample without embedded quantum dots.

In addition to the overview of the dislocation distribution, a

detailed analysis of the threading dislocation filtering mechanism was conducted according to the zoomed-in TEM images in Fig. 4. In general, the strain fields of QD dislocation filters can act upon any threading dislocation that moves perpendicular to them and impose an attractive force ( $F_d$ ) between mobile TDs to overcome the energy barrier for them to glide and interact with each other [20]. The interaction process between TDs depends on the highly stress-related capture radius  $R$  [21]. Only dislocations that pass within the distance  $R$  are energetically favorable to meet and react with each other, leading to annihilation or combination into a single mobile/sessile TD, as shown in Fig. 4(b). The capture radius  $R$  is influenced by the strain-thickness product ( $\xi^*h$ ). When the layer is closer to the critical  $\xi^*h$  value, the radius  $R$  reaches its maximum value ( $\sim$  tens to hundreds of nm). The misfit strain  $\xi$  and the capture radius  $R$  of InAs QDs are larger compared with conventional 2D SLS. This greatly favors the effectiveness of dislocation bending towards the sample edge, rather than propagating perpendicularly to the top surface. Fig. 4(a) shows the dislocations bent at the interface of the QDs and the InP beneath. In Fig. 4(b), the “termination” of dislocations at the surface of QDs could be a result of either the formation of a dislocation loop at the QD surface or the formation of a dislocation of opposite Burgers vector which annihilates the preexisting dislocation [22]. However, some of the planar defects such as SFs are not affected by the QDs and propagate up to the top surface of the InP, as evidenced in Fig. 4(c)–(e). This may imply that the QDs are less effective in filtering the SFs. From the high-resolution image in Fig. 4(d), it can be noted that some QDs are diamond shaped, with a diameter of  $\sim$ 50 nm. These large QDs are formed due to the bumpy surface of the InP-on-Si compliant substrate, which may generate new defects. Therefore, a smoother InP growth front is desirable for the deposition of dense and uniform QDs. Additionally, as observed in Fig. 4(e), the surrounding strain field of the lower QDs will function as nucleation sites for the subsequent upper QDs deposition, thus most of the QDs are vertically aligned.

Finally, room-temperature photoluminescence (RT-PL) spectra on quarter wafers of InP-on-Si samples were measured. A continuous wave (CW) 514 nm Ar ion laser at two different pump power regimes (2 mW and 0.2 mW, respectively) with a focused spot diameter of  $\sim$ 3.5  $\mu$ m was used as excitation. In Fig. 5(a) and (b), an apparent intensity enhancement is noted after the insertion of the QDs. Reduced PL intensity at RT is an indication of dislocations as non-radiative recombination centers. Fig. 5(c)–(e) plot the integrated intensity, peak intensity and full-width at half-maximum values (FWHM) values of the two samples as a function of the excitation power. In both excitation power regimes, the FWHM values of the InP-on-Si with QDs insertion are smaller, together with higher peak and integrated intensities, suggesting the effect of dislocation filtering resulting in better crystalline quality. However, a dislocation density in the order of  $10^8/\text{cm}^2$  is still considered high for practical applications of reliable laser sources. Therefore, the next critical step is to further reduce the dislocation density by optimizing the dislocation filter structures. Stacking more QD layers (maximized between 20 and 30 layers) without exceeding critical thickness and growing larger dots with a higher density are always beneficial. Combining the QD filters with other defect trapping/filtering techniques, such as thermal cycle annealing and patterned growth, could also be explored.

In conclusion, we investigated the dislocation filtering effects of multi-layer InAs/InAlGaAs quantum dots inserted into an InP-on-Si system. The dislocation filtering mechanism was analyzed and the filtering efficiency was evaluated. Furthermore, a smoother surface was obtained owing to the introduction of these filter layers. This work thus marks a promising step towards the monolithic integration of InP-based optoelectronic devices on a silicon manufacturing platform.

## Acknowledgements

This work was supported in part by Grants (614312 and 16212115) from the Research Grants Council of Hong Kong. The authors would like to thank C. W. Tang for the assistance in growth, and the MCPF and NFF of HKUST for their technical support. Helpful discussions with S. Zhu, C. Liu and Y. Han are also acknowledged.

## References

- [1] Y. Sun, C. Junesand, W. Metaferia, H. Kataria, N. Julian, J.E. Bowers, G. Pozina, L. Hultman, S. Lourduoss, Optical and structural properties of sulfur-doped ELOG InP on Si, *J. Appl. Phys.*, 117 (2015) 215303.
- [2] M.Z.M. Khan, T.K. Ng, B.S. Ooi, Self-assembled InAs/InP quantum dots and quantum dashes: material structures and devices, *Prog. Quant. Electron.*, 38 (2014) 237–313.
- [3] H. Kataria, W. Metaferia, C. Junesand, C. Zhang, N. Julian, J.E. Bowers, S. Lourduoss, Simple epitaxial lateral overgrowth process as a strategy for photonic integration on silicon, *IEEE J. Sel. Top. Quant. Electron.*, 20 (2014) 380–386.
- [4] Y. Ababou, P. Desjardins, A. Chennouf, R. Leonelli, D. Hetherington, A. Yelon, G. L'Espérance, R.A. Masut, “Structural and optical characterization of InP grown on Si (111) by metalorganic vapor phase epitaxy using thermal cycle growth, *J. Appl. Phys.*, 80 (1996) 4997–5005.
- [5] N. Mukherjee, J. Boardman, B. Chu-Kung, G. Dewey, N. Julian, A. Eisenbach, J. Fastenau, J. Kavalieros, W. Liu, D. Lubyshv, M. Metz, MOVPE III–V material growth on silicon substrates and its comparison to MBE for future high performance and low power logic applications, *IEEE Electron Devices Meet. (IEDM)* (2011) 35.1.1–35.1.4.
- [6] L. Yang, M.T. Bulsara, K.E. Lee, E.A. Fitzgerald, Compositionally-graded InGaAs–InGaP alloys and GaAsSb alloys for metamorphic InP on GaAs, *J. Cryst. Growth*, 324 (2011) 103–109.
- [7] C. Merckling, N. Waldron, S. Jiang, W. Guo, N. Collaert, M. Caymax, E. Vancoille, K. Barla, A. Thean, M. Heyns, Heteroepitaxy of InP on Si (001) by selective-area metal organic vapor-phase epitaxy in sub-50 nm width trenches: the role of the nucleation layer and the recess engineering, *J. Appl. Phys.*, 115 (2014) 023710.
- [8] B. Shi, Q. Li, Y. Wan, K. Ng, X. Zou, C. Tang, K.M. Lau, InAlGaAs/InAlAs MQWs on Si substrate, *IEEE Photon. Tech. Lett.*, 27 (2015) 748–751.
- [9] Q. Li, K.W. Ng, C.W. Tang, K.M. Lau, R. Hill, A. Vert, Defect reduction in epitaxial InP on nanostructured Si (001) substrates with position-controlled seed arrays, *J. Cryst. Growth*, 405 (2014) 81–86.
- [10] K. Samonji, H. Yonezu, Y. Takagi, K. Iwaki, N. Ohshima, J. Shin, K. Pak, Reduction of threading dislocation density in InP-on-Si heteroepitaxy with strained short-period superlattices, *Appl. Phys. Lett.* 69 (1996) 100–102.
- [11] S. Chen, W. Li, J. Wu, Q. Jiang, M. Tang, S. Shutts, S. Elliott, A. Sobiesierski, A. Seeds, I. Ross, Electrically pumped continuous-wave III–V quantum dot lasers on silicon, *Nat. Photonics* 10 (2016) 307–311.
- [12] S. Naritsuka, T. Nishinaga, M. Tachikawa, H. Mori, InP layer grown on (001) silicon substrate by epitaxial lateral overgrowth, *Jpn. J. Appl. Phys.*, 34 (1995) L1432.
- [13] C. Junesand, H. Kataria, W. Metaferia, N. Julian, Z. Wang, Y. Sun, J.E. Bowers, G. Pozina, L. Hultman, S. Lourduoss, Study of planar defect filtering in InP grown on Si by epitaxial lateral overgrowth, *Opt. Mat. Express* 3 (2013) 1960–1973.
- [14] P. Bhattacharya, Z. Mi, J. Yang, D. Basu, D. Saha, Quantum dot lasers: from promise to high-performance devices, *J. Cryst. Growth*, 311 (2009) 1625–1631.
- [15] Z. Mi, J. Yang, P. Bhattacharya, G. Qin, Z. Ma, High-performance quantum dot lasers and integrated optoelectronics on Si, *P. IEEE*, 97 (2009) 1239–1249.
- [16] C.W. Tang, Z. Zhong, K.M. Lau, Hetero-epitaxy of III–V compounds by MOCVD on silicon substrates, *ECS Trans.*, 28 (2010) 227–231.
- [17] B. Shi, K.M. Lau, Enhanced optical properties of InAs/InAlGaAs/InP quantum dots grown by metal-organic chemical vapor deposition using a double-cap technique, *J. Cryst. Growth*, 433 (2016) 19–23.
- [18] A. Hospodková, J. Pangráč, J. Vyskočil, M. Zíková, J. Oswald, P. Komninou, E. Hulicius, Growth of InAs/GaAs quantum dots covered by GaAsSb in multiple structures studied by reflectance anisotropy spectroscopy, *J. Cryst. Growth*, 414 (2015) 156–160.
- [19] I. George, F. Becagli, H. Liu, J. Wu, M. Tang, R. Beanland, Dislocation filters in GaAs on Si, *Semicond. Sci. Tech.*, 30 (2015) 114004.
- [20] T. Ward, A.M. Sánchez, M. Tang, J. Wu, H. Liu, D.J. Dunstan, R. Beanland, Design rules for dislocation filters, *J. Appl. Phys.* 116 (2014) 063508.
- [21] R.S. Fertig, S.P. Baker, Capture cross-section of threading dislocations in thin films, *Mat. Sci. Eng.: A* 551 (2012) 67–72.
- [22] J. Yang, P. Bhattacharya, Z. Mi, High-performance  $\text{In}_{0.5}\text{Ga}_{0.5}\text{As}/\text{GaAs}$  quantum-dot lasers on silicon with multiple-layer quantum-dot dislocation filters, *IEEE Trans. Electron Devices* 54 (2007) 2849–2855.